The Astrophysical Journal, 812:143 (8pp), 2015 October 20 doi:10.1088/0004-637X/812/2/143

PULSAR J0453+1559: A DOUBLE NEUTRON STAR SYSTEM WITH A LARGE MASS ASYMMETRY

J. G. Martinez[1,2], K. Stovall[1,3], P. C. C. Freire[2], J. S. Deneva[4], F. A. Jenet[1], M. A. McLaughlin[5], M. Bagchi[5,6], S. D. Bates[5], and A. Ridolfi[2]

[1] Center for Advanced Radio Astronomy, University of Texas at Brownsville, One West University Boulevard, Brownsville, TX 78520, USA
[2] Max-Planck-Institut für Radioastronomie, Auf dem Hügel 69, D-53121 Bonn, Germany
[3] Department of Physics and Astronomy, University of New Mexico, Albuquerque, NM 87131, USA
[4] National Research Council, Resident at the Naval Research Laboratory, Washington, DC 20375, USA
[5] Department of Physics and Astronomy, West Virginia University, 111 White Hall, Morgantown, WV 26506, USA
[6] The Institute of Mathematical Sciences, 4th Cross Road3, CIT Campus Taramani, Chennai 600 113, India
Received 2015 April 28; accepted 2015 August 31; published 2015 October 19

ABSTRACT

To understand the nature of supernovae and neutron star (NS) formation, as well as binary stellar evolution and their interactions, it is important to probe the distribution of NS masses. Until now, all double NS (DNS) systems have been measured as having a mass ratio close to unity ($q \geqslant 0.91$). Here, we report the measurement of the individual masses of the 4.07-day binary pulsar J0453+1559 from measurements of the rate of advance of periastron and Shapiro delay: the mass of the pulsar is $M_{\rm p} = 1.559 \pm 0.005\ M_{\odot}$ and that of its companion is $M_{\rm c} = 1.174 \pm 0.004\ M_{\odot}$; $q = 0.75$. If this companion is also an NS, as indicated by the orbital eccentricity of the system ($e = 0.11$), then its mass is the smallest precisely measured for any such object. The pulsar has a spin period of 45.7 ms and a spin period derivative of $\dot{P} = (1.8616 \pm 0.0007) \times 10^{-19}$ s s^{-1}; from these, we derive a characteristic age of $\sim 4.1 \times 10^9$ years and a magnetic field of $\sim 2.9 \times 10^9$ G, i.e., this pulsar was mildly recycled by the accretion of matter from the progenitor of the companion star. This suggests that it was formed with (very approximately) its current mass. Thus, NSs form with a wide range of masses, which is important for understanding their formation in supernovae. It is also important for the search for gravitational waves released during an NS–NS merger: it is now evident that we should not assume that all DNS systems are symmetric.

Key words: gravitational waves – pulsars: general – pulsars: individual (J0453+1559)

1. INTRODUCTION

Double neutron star (DNS) systems are rare and valuable physical laboratories that can be used to precisely test gravity theories. The first such system, PSR B1913+16, provided evidence for orbital decay due to the emission of gravitational waves, as predicted by general relativity (GR; Hulse & Taylor 1975 and Taylor & Weisberg 1982). Since the discovery of PSR B1913+16, nine additional DNS systems have been discovered in the Galaxy (see Table 1), including one such system in which both neutron stars (NSs) have been detected as radio pulsars, PSRs J0737−3039A and B (Burgay et al. 2003, Lyne et al. 2004). This system provides one of the best available tests of GR and alternative theories of gravity in the strong-field regime (Kramer et al. 2006).

DNS systems begin as two high-mass stars. The higher-mass star will undergo a supernova explosion resulting in an NS and a high-mass companion. Prior to the supernova of the companion, there is typically a period of mass transfer from the companion to the NS, and the system can be detected as a high-mass X-ray binary. Eventually, the companion will undergo a supernova explosion, leaving behind two NSs: the older might be detected as a mildly recycled pulsar which was spun up by accretion from the progenitor of the younger star, and the younger might be detected as a normal pulsar. In the rare case that the system survives both supernovae, the result is a DNS (see Lorimer 2008 and references therein).

In this letter, we report the timing solution for PSR J0453+1559, a pulsar discovered in the Arecibo 327 MHz Drift Pulsar Survey (Deneva et al. 2013). At the time of writing this survey has discovered a total of 62 pulsars and rotating radio transients. As reported by Deneva et al. (2013), PSR J0453+1559 has a spin period of 45.7 ms, a dispersion measure (DM) of 30.3 pc cm^{-3}, an orbital period of 4.07 days, and a massive companion.

In Section 2, we describe the observations, data reduction, and the derivation of the timing solution. In Section 3, we present the timing parameters of this new system. In Section 4, we conclude with a discussion of the significance of the timing parameters.

2. OBSERVATIONS AND DATA REDUCTION

PSR J0453+1559 was observed with the L-wide receiver of the 305-m Arecibo radio telescope 45 times over 2.5 years using the Puerto Rico Ultimate Pulsar Processing Instrument (PUPPI, a clone of the Green Bank Ultimate Pulsar Processing Instrument, GUPPI)[7] as a back-end, which allows simultaneous processing of the $\Delta f = 600$ MHz bandwidth provided by the receiver (from 1130 to 1730 MHz) with a system temperature $T_{\rm sys} = 30$ K and a gain $G = 10$ K Jy^{-1}. The first six months' observations were taken in search mode with 2048 channels, a time resolution $T_{\rm res}$ of 40.96 μs, two polarizations ($n_{\rm p} = 2$), and basically no sensitivity degradation due to digitization ($\beta \simeq 1$), since PUPPI digitizes the antenna voltages with 8 bits. After derivation of a phase-connected timing solution, these were dedispersed and folded using `DSPSR`,[8] (van Straten & Bailes 2011), producing 1024-bin profiles.

This initial timing ephemeris made it possible to conduct all of the subsequent observations in coherent fold mode (with 512 channels, 2048 phase bins, and 4 Stokes parameters), which coherently dedisperses and folds the data online, optimally

[7] http://safe.nrao.edu/wiki/bin/view/CICADA/GUPPISupportGuide
[8] http://dspsr.sourceforge.net/

Table 1
Double Neutron Star Systems Known in the Galaxy

Pulsar	Period (ms)	P_b (days)	x (lt-s)	e	M ($M_\odot$)	M_p ($M_\odot$)	M_c ($M_\odot$)	References
J0737–3039A	22.699	0.102	1.415	0.0877775(9)	2.58708(16)	1.3381(7)	1.2489(7)	(1)
J0737–3039B	2773.461	⋯	1.516	⋯	⋯	⋯	⋯	⋯
J1518+4904	40.935	8.634	20.044	0.24948451(3)	2.7183(7)	⋯	⋯	(2)
B1534+12	37.904	0.421	3.729	0.27367740(4)	2.678463(4)	1.3330(2)	1.3454(2)	(3)
J1753–2240	95.138	13.638	18.115	0.303582(10)	⋯	⋯	⋯	(4)
J1756–2251	28.462	0.320	2.756	0.1805694(2)	2.56999(6)	1.341(7)	1.230(7)	(5)
J1811–1736	104.1	18.779	34.783	0.82802(2)	2.57(10)	⋯	⋯	(6)
J1829+2456	41.009	1.760	7.236	0.13914(4)	2.59(2)	⋯	⋯	(7)
J1906+0746[a]	144.073	0.166	1.420	0.0852996(6)	2.6134(3)	1.291(11)	1.322(11)	(8)
B1913+16	59.031	0.323	2.342	0.6171334(5)	2.8284(1)	1.4398(2)	1.3886(2)	(9)
J1930–1852	185.520	45.060	86.890	0.39886340(17)	2.59(4)	⋯	⋯	(10)
J0453+1559	45.782	4.072	14.467	0.11251832(4)	2.734(3)	1.559(5)	1.174(4)	This letter
Globular Cluster Systems								
J1807–2500B[a]	4.186	9.957	28.920	0.747033198(40)	2.57190(73)	1.3655(21)	1.2064(20)	(12)
B2127+11C	30.529	0.335	2.518	0.681395(2)	2.71279(13)	1.358(10)	1.354(10)	(13)

Note.
[a] There is some uncertainty on whether these systems are DNSs.
References. (1) Burgay et al. (2003) and Kramer et al. (2006), (2) Janssen et al. (2008), (3) Wolszczan (1991) and Fonseca et al. (2014), (4) Keith et al. (2009), (5) Faulkner et al. (2005) and Ferdman et al. (2014), (6) Corongiu et al. (2007), (7) Champion et al. (2004, 2005), (8) Lorimer et al. 2006 and van Leeuwen et al. (2015), (9) Hulse & Taylor (1975) and Weisberg et al. (2010), (10) Swiggum et al. (2015), (12) Lynch et al. (2012), (13) Anderson et al. (1989) and Jacoby et al. (2006).

removing the dispersive effects of the interstellar medium. These observations have improved the signal-to-noise ratio (S/N) because they benefit from the better pointing position derived from the timing solution. The pulse profile is displayed in Figure 1. The main pulse has a sharp feature that contributes significantly to the good timing precision of this pulsar discussed in Section 3.

The dedispersed pulse profiles obtained when averaging the 11-minute blocks of timing data produced by PUPPI are then calibrated using the noise diode observations taken with (almost) every single observation. The resulting calibrated pulse profiles are then cross-correlated with the low-noise template displayed in Figure 1 using the procedure described in Taylor (1992) and implemented in the PSRCHIVE software (Hotan et al. 2004; van Straten et al. 2012). This resulted in 868 usable topocentric pulse times of arrival (TOAs).

We then used TEMPO[9] to correct the TOAs using the Arecibo telescope's clock corrections and to convert them to the Solar System barycenter. To do this, the motion of the radio telescope relative to the Earth was calculated using data from the International Earth Rotation Service, and to the barycenter using the DE421 solar system ephemeris.[10] Finally, the difference between the measured TOAs and those predicted by a model of the spin and the orbit of the pulsar is minimized by TEMPO, by varying the parameters in the model. The parameters that best fit the data are presented in the first column of Table 2. To model the orbit, we used the DDGR model described by Damour & Deruelle (1985) and Damour & Deruelle (1986), which assumes the validity of GR in the description of the orbital motion of the system and uses as parameters the total mass of the system M and the companion mass M_c.

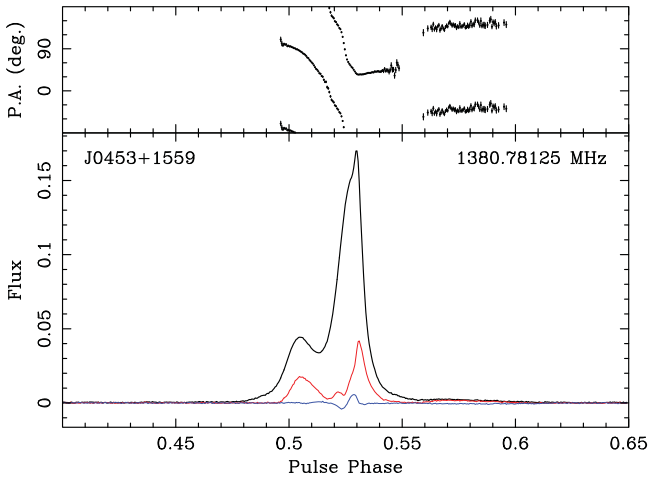

Figure 1. Pulse profile for PSR J0453+1559 in the L band (1170–1730 MHz), obtained by averaging the best detections of the pulsar. The black line indicates the total intensity, the red line is the amplitude of linear polarization, and the blue line is the amplitude of the circular polarization. In the top panel, we depict the position angle of the linear polarization where a clear polarization swing and a sudden jump between orthogonal modes is clearly visible.

The residuals (TOAs minus model predictions) associated with this DDGR model are displayed in Figure 2. There are some short-term trends in the residuals that point toward unmodeled systematics. For this reason, we added 2.5 μs (the approximate amplitude of these systematics) in quadrature to the TOA uncertainties, and in this way the reduced χ^2 is close to 1.0 both for TOAs with large and small uncertainties. The amplitude of the systematics is smaller for the data with polarization calibration, which suggests imperfect polarization calibration might be a cause of the systematics in the uncalibrated data. The residual root mean square is 4 μs, which represents a fraction of 8.7×10^{-5} of the spin period.

[9] http://tempo.sourceforge.net/
[10] ftp://ssd.jpl.nasa.gov/pub/eph/planets/ioms/de421.iom.v1.pdf

Table 2
Timing Parameters for PSR J0453+1559

Observation Parameters		
Fitting program	TEMPO	TEMPO2
Time units	TDB	TCB
Solar system ephemeris	DE421	DE421
Reference epoch (MJD)	56400	56400
Span of timing data (MJD)	56339–57207	56339–57207
Number of TOAs	868	868
rms residual (μs)	3.96	3.88
Solar n_0 (cm^{-3})	0.0	0.0
Spin and Astrometric Parameters		
R.A., α (J2000)	04:53:45.41372(4)	04:53:45.41368(5)
decl., δ (J2000)	+15:59:21.3055(50)	+15:59:21.3063(59)
Proper motion in R.A., μ_α (mas yr^{-1})	−5.4(4)	−5.5(5)
Proper motion in decl., μ_δ (mas yr^{-1})	−5.3(3.6)	−6.0(4.2)
Pulsar period, P (s)	0.045781816163093(3)	0.045781816729515(33)
Period derivative, $\dot{P}$ (10^{-18} s s^{-1})	0.18616(7)	1.8612(8)
Dispersion measure, DM (pc cm^{-3})	30.30527(26)	30.3053(3)
Binary Parameters		
Orbital model	DDGR	DDH
Orbital period, P_b (days)	4.072468588(4)	4.072468649(4)
Projected semimajor axis of the pulsar orbit, x (lt-s)	14.466798(5)	14.4667896(42)
Epoch of periastron, T_0 (MJD)	56344.0029907(6)	56344.0031965(9)
Orbital eccentricity, e	0.11251832(4)	0.11251844(8)
Longitude of periastron, ω (°)	223.06953(6)	223.06965(8)
Relativistic Parameters and Masses		
Rate of advance of periastron, $\dot{\omega}$ (° yr^{-1}) ..	0.0379412 (d)	0.03793(3)
Orthometric amplitude, h_3 (μs) ..	⋯	3.07(25)
Orthometric ratio, ς ..	⋯	0.709(40)
Total mass, M ($M_\odot$) ..	2.734(4)	2.733(4) (d)
Companion mass, M_c ($M_\odot$) ..	1.174(4)	1.172(4) (m)
Derived Parameters		
Mass function, f ($M_\odot$) ..	0.19601284(22)	0.19601248(4)
Pulsar mass, M_p ($M_\odot$) ..	1.559(5)	1.560(5) (m)
Orbital inclination, i (°) ..	75.2699	$75.7^{+0.7}_{-0.8}$ (m)
Galactic longitude, l ..	184.1245	
Galactic latitude, b ..	−17.1369	
DM-derived distance, d (kpc) ..	1.1	
Galactic height, z (kpc) ..	−0.29	
Transversal velocity, $v_\perp$ (km s^{-1}) ..	40	
Kinematic correction to $\dot{P}$, (10^{-18} s s^{-1}) ..	0.0089	
Intrinsic $\dot{P}$, (10^{-18} s s^{-1}) ..	≃0.177(2)	
Surface magnetic field strength, B_0 (10^9 Gauss) ..	2.9	
Characteristic age, τ_c (Gyr) ..	4.1	

Notes. Numbers in parentheses represent 1σ uncertainties in the last digits as determined by TEMPO, scaled such that the reduced $\chi^2 = 1$. Note that the timing parameters are given in two different timescales, TDB and TCB. (d) indicates a parameter that is derived in one model, but fitted directly in the other. (m) parameter derived from the Bayesian analysis described in the text. The distance is derived from the DM using the Cordes & Lazio (2002) model of the Galactic electron density with a ∼25% uncertainty.

In order to double check the results, we used TEMPO2 (Hobbs et al. 2006 and Edwards et al. 2006) and the DDH model described by Freire & Wex (2010), which like the DD (but unlike the DDGR model) allows a theory-independent fit for the detectable post-Keplerian (PK) parameters: in this case, the rate of advance of periastron ($\dot{\omega}$) and two parameters that provide an optimized description of the Shapiro delay, the orthometric amplitude (h_3) and the orthometric ratio (ς). As we will see, the measurement of the PK parameters is important because it allows an understanding of the precision of the mass measurements derived from the DDGR model and also a double check on its accuracy.

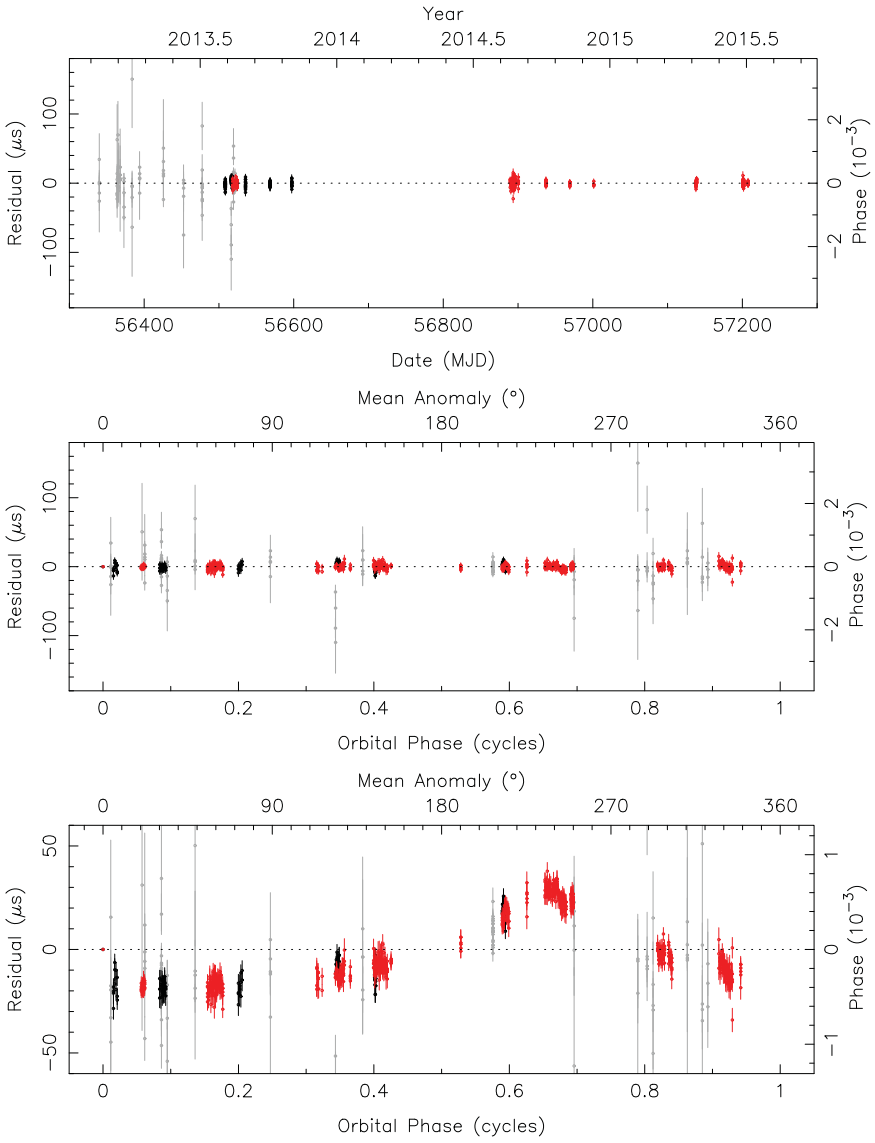

Figure 2. Top plot is the timing solution for PSR J0453+1559, timing residuals (measured pulse arrival times—model pulse arrival times) as a function of MJD. The middle and bottom plots show the timing residuals vs. orbital phase of the J0453+1559 system. The bottom plot shows the magnitude of the Shapiro Delay as a function of orbital phase, derived with the same Keplerian orbital parameters from the DDGR ephemeris in Table 2. The color of the timing residuals are categorized as follows: gray is the search mode data, black is the coherent fold mode uncalibrated data, and red is coherent fold mode calibrated data.

3. RESULTS

The pulsar's ephemeris in Table 2 includes a precise position in the sky, which allows for optical follow-up. No optical counterpart to the system is detectable in the online DSS2 optical survey, either in the red or blue filters, or in the 2MASS survey.

We can detect the proper motion in R.A., and have useful limits for the proper motion in decl. We can derive a total proper motion of $\mu = (7.0 \pm 2.5)$ mas yr^{-1}. The ephemeris also includes the pulsar's spin period (P) and its derivative ($\dot{P}$). Taking into account the effect of the proper motion (Shklovskii 1970) and Galactic acceleration (Damour & Taylor 1991) on $\dot{P}$ at the DM-derived distance of 1.1 kpc, we obtain an intrinsic $\dot{P}$ of $1.77(2) \times 10^{-19}$ s s^{-1}. From this, we derive a characteristic age of $\sim 4.1 \times 10^9$ years and a surface inferred magnetic field of 2.9×10^9 G. These numbers are similar to what we observe for other recycled pulsars with massive companions, and they indicate that this pulsar was mildly recycled by the accretion of matter from the progenitor of the current companion star (Tauris et al. 2012).

The ephemeris also includes very precise orbital parameters. The orbital period P_b is 4.07 days, i.e., this is not a tight system where we might be able to measure all PK parameters precisely: the Einstein delay (γ) will take a long time to measure and it will correlate strongly with the kinematic $\dot{x}$ term that arises from the proper motion (Arzoumanian et al. 1996 and Kopeikin 1996); the orbital decay due to the emission of gravitational waves ($\dot{P}_b$) will be extremely small and masked by much larger kinematic contributions (Shklovskii 1970 and Damour & Taylor 1991). The projected semimajor axis of the pulsar's orbit x is 14.5 lt-s; from this, we can derive the Keplerian mass function:

$$f(M_p, M_c) = \frac{(M_c \sin i)^3}{(M_p + M_c)^2} = \frac{4\pi^2 x^3}{T_\odot P_b^2} = 0.1960128(2)\, M_\odot, \quad (1)$$

where $T_\odot = G\,M_\odot\,c^{-3} = 4.925490947\,\mu$s is the solar mass ($M_\odot$) in time units ($c$ is the speed of light and G is Newton's gravitational constant), i is the angle between the plane of the orbit and the plane of the sky, and the pulsar and companion masses M_p and M_c, are in solar masses. If we assume a mass of 1.4 $M_\odot$ for the pulsar and maximum and median orbital inclinations ($i = 90°$, $60°$), then we obtain minimum and median companion masses of 1.05 and 1.30 $M_\odot$, i.e., the companion is relatively massive.

Given the orbital eccentricity ($e = 0.11$), the companion is very likely to be an NS—if it had evolved into a massive white dwarf star, then there would be no sudden mass loss associated with a supernova explosion and the system would have retained the circular orbit characteristic of compact accreting systems. This is consistent with the non-detection of an optical counterpart of the system in any of the optical catalogs. However, the high eccentricity does not entirely settle the matter: the recent discovery of a recycled pulsar with a massive ($\sim 1 M_\odot$) companion PSR J1727–2946(Lorimer et al. 2015) and an orbital eccentricity of 0.0456 bridges the previously observed eccentricity gap between systems with NS and massive WD companions. In the remainder of this paper, we will assume, with caution, that the companion is an NS.

The pulsar's orbital eccentricity allows a detection of the advance of periastron, $\dot{\omega}$. If both components are compact, as is implied by the optical non-detection, then this is given by

$$\dot{\omega} = \dot{\omega}_{\rm GR} + \dot{\omega}_{\rm K}. \quad (2)$$

The second term $\dot{\omega_{\rm K}}$ is caused by the change in viewing geometry due to the proper motion μ (Damour & Taylor 1991):

$$\left|\dot{\omega}_{\rm K}\right| = \left|\frac{\mu}{\sin i}\cos\left(\Theta_\mu - \Omega\right)\right| \leqslant 3.65 \times 10^{-6}\,{\rm deg\,yr^{-1}}, \quad (3)$$

where Θ_μ is the position angle (PA) of the proper motion and Ω is the PA of the line of nodes (the intersection of the orbital plane with the plane of the sky). This term is currently one order of magnitude smaller than the experimental uncertainty in the measurement of $\dot{\omega}$. Thus $\dot{\omega}_{\rm GR} \simeq \dot{\omega}$.

The first term depends only on the Keplerian orbital parameters, which are already known precisely, and the total mass of the binary M. Thus, M can be derived from a measurement of $\dot{\omega}_{\rm GR}$ (Weisberg et al. 1981):

$$M = \frac{1}{T_\odot}\left[\frac{\dot{\omega}_{\rm GR}}{3}\left(1 - e^2\right)\right]^{\frac{3}{2}}\left(\frac{P_b}{2\pi}\right)^{\frac{5}{2}}. \quad (4)$$

This yields $M = 2.734 \pm 0.003 M_\odot$. As we can see in Table 1, this is within the mass range of currently known DNS systems.

We also measure the Shapiro delay with some precision. In the DDH solution, h_3 and ς are measured with 10 and 17σ significance. This in principle allows a measurement of the system masses using the Shapiro delay alone.

In order to estimate the masses from the Shapiro delay, we sampled the quality of the fit for a wide region in the M_c–cos i plane, depicted in the left panel of Figure 3. For each point in this plane, we calculate the Shapiro delay parameters assuming GR to be the correct theory of gravity and then introduce them into the timing solution, keeping them fixed and fitting for all other timing parameters. The quality of the fit is quantified by the χ^2 of the resulting solution; the lower this is, the better the fit. From this χ^2 map, we derive a two-dimensional (2D) probability distribution function (pdf) using the Bayesian specification in Splaver et al. (2002). This is then converted to a similar 2D pdf in the M_c–M_p plane (right panel) using Equation (1). The black contours of both panels include 68.27% and 95.45% of the total probability of each pdf. We then marginalize the 2D pdfs to derive one-dimensional (1D) pdfs for M_c, cos i, and M_p; the latter are presented in the top and right panels in black. They allow for a wide (and rather uninteresting) range of masses for the pulsar and the companion, i.e., just by itself, the Shapiro delay does not provide useful mass constraints.

The precision of these mass estimates increases by two orders of magnitude if for each point in the M_c–cos i plane we fix the Shapiro delay parameters *and* assume that $\dot{\omega}$ is due only to the effects of GR (using Equation (4)). As before, we then fit for all other timing parameters, store the values of χ^2, and calculate a second 2D pdf. The latter is illustrated in Figure 3 by the red regions, which include 95.4% of its total probability. Marginalizing this second pdf along the different axes, we obtain for the medians and 1σ percentiles the following values: $M_p = 1.559 \pm 0.005\ M_\odot$, $M_c = 1.172 \pm 0.004\ M_\odot$, and $i = 75.7^{+0.7}_{-0.8}°$, respectively. This is consistent with the masses provided by the DDGR model in `TEMPO`.

3.1. Search for the Companion as a Radio Pulsar

In order to search for radio pulsations from the companion, we used the early observations, which were taken in search mode. The precise measurement of the masses of the two NSs in the system allows us to derive a complete ephemeris for the companion NS, except for the spin parameters. This ephemeris was used to resample the time series (dedispersed at the DM of the known pulsar) for the reference frame of the companion. This way, we removed any possible losses in sensitivity due to the companion acceleration. We then used the PRESTO pulsar search code[11] to search for periodic signals in the resampled time series, and used it to fold all of the candidates, which were then inspected visually. No pulsations coming from the companion were detected.

To estimate the upper limit on the companion's pulsed mean flux density in our line of sight, $S_{\rm max}$, we used the radiometer equation (Lorimer & Kramer 2004), using the parameters of the search observations and accounting for dispersive smearing at the DM of the system and a minimum S/N of 10. For L-band observations, the parameters are those reported in Section 2, whereas at 327 MHz we have $T_{\rm sys} = 113$ K, $G = 11\,{\rm K\,Jy^{-1}}$, and $\Delta f = 60$ MHz. In the L-band, the longest observation had a length of $t_{\rm obs} = 6300$ s, whereas for only the 327 MHz observation available to us $t_{\rm obs} = 240$ s.

Figure 4 shows $S_{\rm max}$ as a function of the unknown companion spin period, $P_{\rm com}$, for intrinsic duty cycles of 1%, 5%, and 10%. For the range of expected spin periods of the companion ($P_{\rm com} \gtrsim 0.1$ s), $S_{\rm max,1400} \lesssim 4\,\mu$Jy, and $S_{\rm max,327} \lesssim 202\,\mu$Jy. Given the estimated distance of 1.0 kpc, these translate into pseudo-luminosities of $L_{\rm max,1400} \lesssim 4\ \mu{\rm Jy\,kpc^2}$ and $L_{\rm max,327} \lesssim 202\ \mu{\rm Jy\,kpc^2}$, respectively. No pulsar in the ATNF catalog[12] has an estimated L_{1400} as low as this.

[11] http://www.cv.nrao.edu/~sransom/presto/
[12] http://www.atnf.csiro.au/people/pulsar/psrcat/

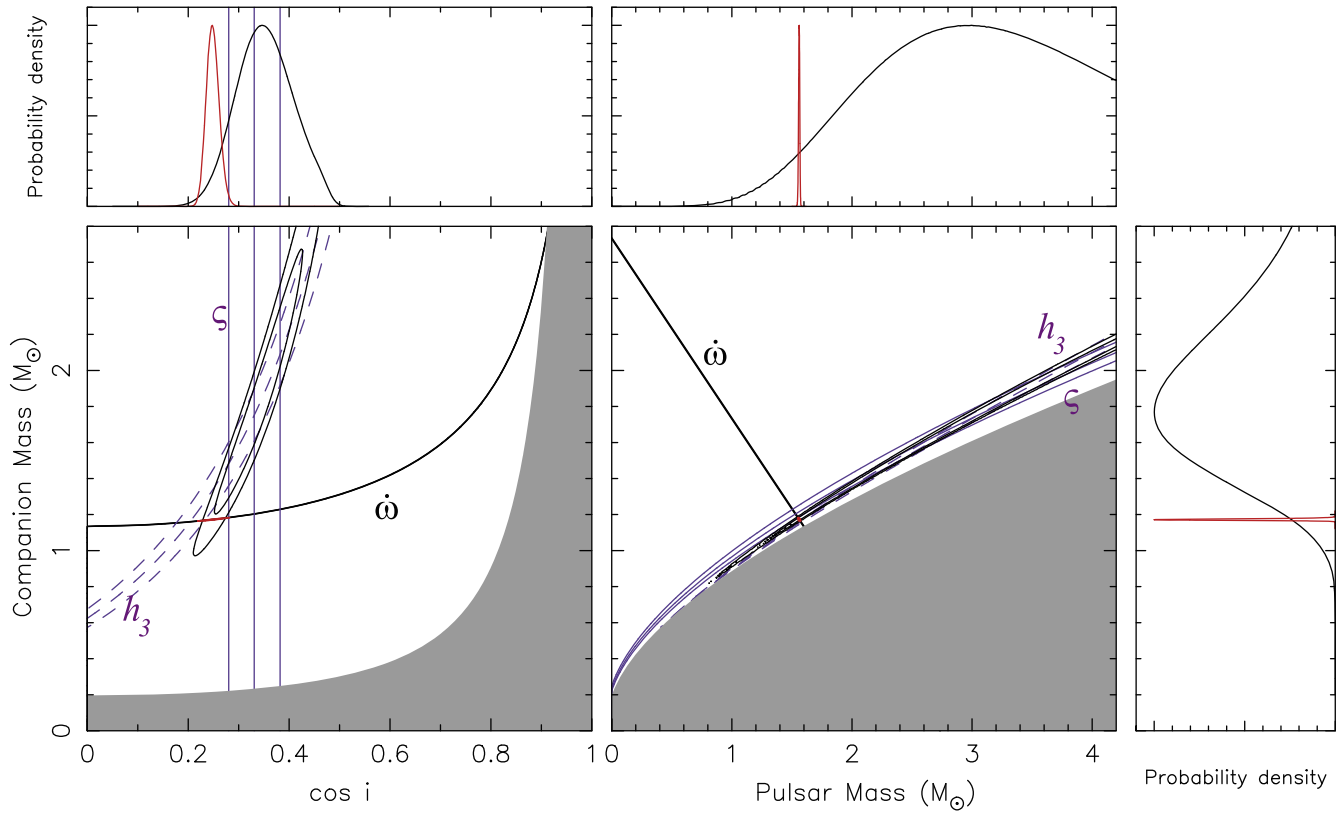

Figure 3. Current constraints from the timing of PSR J0453+1559. Each triplet of lines corresponds to the nominal and $\pm 1\sigma$ uncertainties of the post-Keplerian parameters measured using the DDH model in TEMPO2 (see Table 2), which are the rate of advance of periastron $\dot{\omega}$, the orthometric ratio of the Shapiro delay ς, and the orthometric amplitude of the Shapiro delay, h_3 (Freire & Wex 2010). The contour levels contain 68.27% and 95.45% of the 2D probability density functions (pdfs) derived from the quality of the timing solution at each point of the M_c–cos i plane using only the Shapiro delay (black) and Shapiro delay plus the assumption that the $\dot{\omega}$ is due only to the effects of GR (red). Left: M_c–cos i plane. The gray region is excluded by the physical constraint $M_p > 0$. Right: M_c–M_p plane. The gray region is excluded by the mathematical constraint $\sin i \leqslant 1$. Top and right panels: pdfs for cos i, M_p, and (on the right) M_c, derived from marginalizing the 2D pdf in the main panel for these quantities. When $\dot{\omega}$ is taken into account (red), the precision of the mass estimates improves by two orders of magnitude.

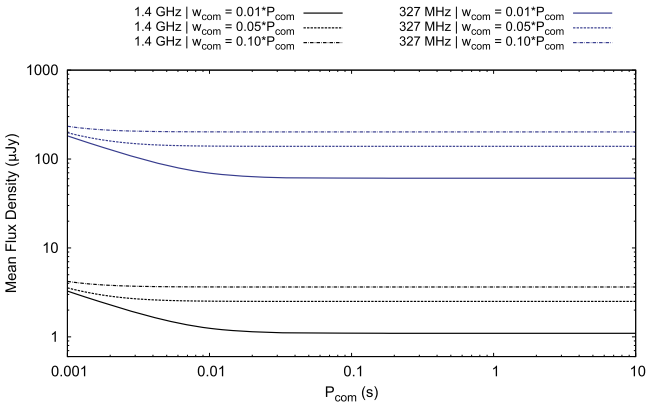

Figure 4. Estimated minimum mean flux density of the companion if detectable with an S/N = 10, as a function of its spin period P_{com} at 1.4 GHz (black lines) and 327 MHz (blue lines). For each frequency, the cases of an intrinsic duty cycle w_{com} of 1% (solid line), 5% (dashed line), and 10% (dotted–dashed line) of P_{com} are shown. In the L band, the parameters used were $t_{obs} = 6300$ s, $T_{sys} = 30$ K, $G = 10$ K Jy^{-1}, $\Delta f = 600$ MHz; at 327 MHz they were $t_{obs} = 240$ s, $T_{sys} = 113$ K, $G = 11$ K Jy^{-1}, $\Delta f = 60$ MHz; at both frequencies $\beta = 1$ and $n_p = 2$. Because the companion was not detected, its mean flux density must be out of our line of sight.

4. DISCUSSION AND CONCLUSIONS

The accretion episode in DNS systems is very short-lived and therefore the mass of the recycled pulsar is only slightly larger than its mass at birth (Tauris et al. 2015). Until now, most well-measured NS masses in DNS systems fell in a narrow range between 1.23 and 1.44 $M_\odot$ (Weisberg et al. 2010 and Faulkner et al. 2005, see Table 1). This has led to speculation that all NSs might be born within this narrow band, and that the large masses observed in some MSPs like PSR J1903+0327 (Freire et al. 2011), PSR J1614−2230 (Demorest et al. 2010), and PSR J0348+0432 (Antoniadis et al. 2013) are due to accretion. However, from an analysis of the evolution of PSR J1614–2230, Tauris et al. (2011) had already suggested that at least some NSs must be born more massive than 1.44 $M_\odot$. The mass of PSR J0453+1559—the largest ever measured in a DNS system (see Table 1)—and that of its companion—the smallest precisely measured for *any* NS—shows that the range of NS birth masses is indeed substantially wider than earlier studies indicated (Thorsett & Chakrabarty 1999 and Özel et al. 2012).

It is interesting to speculate on how the companion might have formed. Its mass is lower than the 1.24 $M_\odot$ measured for the companion of J1756−2251 (Ferdman et al. 2014) and PSRs J1802−2124 (Ferdman et al. 2010) and J0737−3039B (Kramer et al. 2006) that are thought to have formed in electron capture supernovae (ECSN). It is possible that the companion formed instead in an iron core collapse SN, where the core of the progenitor of the companion was stripped of its envelope (Tauris et al. 2015).

The relatively small eccentricity of the system compared to other DNS systems (see Table 1) suggests a relatively small SN kick velocity at birth, which is consistent both with formation via ECSN and an ultra-stripped iron core SN. In this case, the three-dimensional (3D) velocity of the system in the Galaxy should be small in comparison with the general pulsar population. This is consistent with the inferred transverse velocity of $\sim$40 km s^{-1} and the relatively small Galactic height of the system, 0.29 kpc.

The mass asymmetry is also important because it leads to a peculiar behavior during NS–NS mergers, particularly if the mass ratio is less than 0.8. During the merger, the lighter (and larger) NS is tidally disrupted by the smaller, more massive NS. According to recent simulations (Rezzolla et al. 2010; Hotokezaka et al. 2013 and Rosswog 2013), such mergers result in a much larger release of heavy *r*-process elements into space (Just et al. 2015), possibly explaining the heavy element abundances in our Galaxy. However, asymmetric DNSs can only explain heavy element abundances if they form with an orbital period that is small enough for them to merge well within a Hubble time. Pulsar J0453+1559 has a very large merger time, 1.43 Tyr. However, the mass asymmetry measured in this system opens up the possibility that similar asymmetries might eventually be measured for compact DNSs in the future.

This result is also important for searches of gravitational wave emission from NS–NS mergers using ground-based GW detectors (Abbott et al. 2009 and Abadie et al. 2012)—it shows that we should not assume that the components of DNS systems have similar masses. This result justifies particularly searching for DNS systems with lighter NSs, where more computational effort is required, since in this case the inspiral episodes leading to the merger are significantly longer.

In asymmetric DNSs, dipolar gravitational wave emission could theoretically become important at the later stages of the merger; however, this possibility is already significantly constrained by the measurement of the orbital decay of PSR J1738+0333 (Freire et al. 2012) and J0348+0432 (Antoniadis et al. 2013), at least in the framework of Scalar-Tensor theories of gravity. Therefore, GR-derived templates should be a satisfactory approximation to the merger signal of asymmetric DNSs.

J.S.D. was supported by the Chief of Naval Research. P.C.C.F. and A.R. gratefully acknowledge financial support by the European Research Council for the ERC Starting grant BEACON under contract No. 279702. J.G.M. was supported for this research through a stipend from the International Max Planck Research School (IMPRS) for Astronomy and Astrophysics at the Universities of Bonn and Cologne. A.R. is a member of the International Max Planck research school for Astronomy and Astrophysics at the Universities of Bonn and Cologne and acknowledges partial support through the Bonn-Cologne Graduate School of Physics and Astronomy.

This work would not have been possible without the high sensitivity of the Arecibo 305-m radio telescope, the professionalism and dedication of its excellent staff, and the capabilities of the PUPPI back-end, a clone of the GUPPI developed by NRAO and kindly made available to the whole community by its developers, Scott Ransom, Paul Demorest, and the development team at Charlottesville, VA. The Arecibo Observatory is operated by SRI International under a cooperative agreement with the National Science Foundation (AST-1100968), and in alliance with Ana G. Méndez-Universidad Metropolitana, and the Universities Space Research Association.

J.G.M. would like to deeply thank the Arecibo Remote Command Center (ARCC) program in the Center for Advanced Radio Astronomy (CARA) center at the University of Texas at Brownsville. This program provided the the setting and support that allowed this work to be possible. Thank you to the ARCC Executive Committee for your dedication and hard work.

REFERENCES

Abadie, J., Abbott, B. P., Abbott, R., et al. 2012, PhRvD, 85, 082002
Abbott, B. P., Abbott, R., Adhikari, R., et al. 2009, PhRvD, 79, 122001
Anderson, S., Gorham, P., Kulkarni, S., Prince, T., & Wolszczan, A. 1989, IAU Circ., 4772, 1
Antoniadis, J., Freire, P. C. C., Wex, N., et al. 2013, Sci, 340, 448
Arzoumanian, Z., Joshi, K., Rasio, F. A., & Thorsett, S. E 1996, in ASP Conf. Ser. 105, IAU Coll. 160: Pulsars: Problems and Progress, ed. S. Johnston, M. A. Walker & M. Bailes (San Francisco, CA: ASP), 525
Burgay, M., D'Amico, N., Possenti, A., et al. 2003, Natur, 426, 531
Champion, D. J., Lorimer, D. R., McLaughlin, M. A., et al. 2004, MNRAS, 350, L61
Champion, D. J., Lorimer, D. R., McLaughlin, M. A., et al. 2005, MNRAS, 363, 929
Cordes, J. M., & Lazio, T. J. W. 2002, arXiv:0207156
Corongiu, A., Kramer, M., Stappers, B. W., et al. 2007, A&A, 462, 703
Damour, T., & Deruelle, N. 1985, AnIHP, 43, 107
Damour, T., & Deruelle, N. 1986, AnIHP, 44, 263
Damour, T., & Taylor, J. H. 1991, ApJ, 366, 501
Demorest, P. B., Pennucci, T., Ransom, S. M., Roberts, M. S. E., & Hessels, J. W. T. 2010, Natur, 467, 1081
Deneva, J. S., Stovall, K., McLaughlin, M. A., et al. 2013, ApJ, 775, 51
Edwards, R. T., Hobbs, G. B., & Manchester, R. N. 2006, MNRAS, 372, 1549
Faulkner, A. J., Kramer, M., Lyne, A. G., et al. 2005, ApJL, 618, L119
Ferdman, R. D., Stairs, I. H., Kramer, M., et al. 2010, ApJ, 711, 764
Ferdman, R. D., Stairs, I. H., Kramer, M., et al. 2014, MNRAS, 443, 2183
Fonseca, E., Stairs, I. H., & Thorsett, S. E. 2014, ApJ, 787, 82
Freire, P. C. C., Bassa, C. G., Wex, N., et al. 2011, MNRAS, 412, 2763
Freire, P. C. C., & Wex, N. 2010, MNRAS, 409, 199
Freire, P. C. C., Wex, N., Esposito-Farèse, G., et al. 2012, MNRAS, 423, 3328
Hobbs, G. B., Edwards, R. T., & Manchester, R. N. 2006, MNRAS, 369, 655
Hotan, A. W., van Straten, W., & Manchester, R. N. 2004, PASA, 21, 302
Hotokezaka, K., Kiuchi, K., Kyutoku, K., et al. 2013, PhRvD, 87, 024001
Hulse, R. A., & Taylor, J. H. 1975, ApJL, 195, L51
Jacoby, B. A., Cameron, P. B., Jenet, F. A., et al. 2006, ApJL, 644, L113
Janssen, G. H., Stappers, B. W., Kramer, M., et al. 2008, A&A, 490, 753
Just, O., Bauswein, A., Ardevol Pulpillo, R., Goriely, S., & Janka, H.-T. 2015, arXiv:1504.05448
Keith, M. J., Kramer, M., Lyne, A. G., et al. 2009, MNRAS, 393, 623
Kopeikin, S. M. 1996, ApJL, 467, L93
Kramer, M., Stairs, I. H., Manchester, R. N., et al. 2006, Sci, 314, 97
Lorimer, D. R. 2008, LRR, 11, 8
Lorimer, D. R., Esposito, P., Manchester, R. N., et al. 2015, MNRAS, 450, 2185
Lorimer, D. R., & Kramer, M. 2004, Handbook of Pulsar Astronomy (New York: Cambridge Univ. Press)
Lorimer, D. R., Stairs, I. H., Freire, P. C., et al. 2006, ApJ, 640, 428
Lynch, R. S., Freire, P. C. C., Ransom, S. M., & Jacoby, B. A. 2012, ApJ, 745, 109
Lyne, A. G., Burgay, M., Kramer, M., et al. 2004, Sci, 303, 1153
Özel, F., Psaltis, D., Narayan, R., & Santos Villarreal, A. 2012, ApJ, 757, 55
Rezzolla, L., Baiotti, L., Giacomazzo, B., Link, D., & Font, J. A. 2010, CQGra, 27, 114105
Rosswog, S. 2013, RSPTA, 371, 20272
Shklovskii, I. S. 1970, SvA, 13, 562
Splaver, E. M., Nice, D. J., Arzoumanian, Z., et al. 2002, ApJ, 581, 509
Swiggum, J. K., Rosen, R., McLaughlin, M. A., et al. 2015, MNRAS, 451, 2123
Tauris, T. M., Langer, N., & Kramer, M. 2011, MNRAS, 416, 2130
Tauris, T. M., Langer, N., & Kramer, M. 2012, MNRAS, 425, 1601
Tauris, T. M., Langer, N., & Podsiadlowski, P. 2015, MNRAS, 451, 2123
Taylor, J. H. 1992, RSPTA, 341, 117

Taylor, J. H., & Weisberg, J. M. 1982, ApJ, 253, 908
Thorsett, S. E., & Chakrabarty, D. 1999, ApJ, 512, 288
van Leeuwen, J., Kasian, L., Stairs, I. H., et al. 2015, ApJ, 798, 118
van Straten, W., & Bailes, M. 2011, PASA, 28, 1
van Straten, W., Demorest, P., & Oslowski, S. 2012, AR&T, 9, 237
Weisberg, J. M., Nice, D. J., & Taylor, J. H. 2010, ApJ, 722, 1030
Weisberg, J. M., Taylor, J. H., & Fowler, L. A. 1981, SciAm, 245, 74
Wolszczan, A. 1991, Natur, 350, 688